Molecular resolution imaging of protein molecules in liquid using frequency modulation atomic force microscopy

Molecular Resolution Imaging of Protein Molecules in Liquid using Frequency Modulation Atomic Force Microscopy

Hirofumi Yamada*, Kei Kobayashi[1], Takeshi Fukuma†, Yoshiki Hirata[2], Teruyuki Kajita, and Kazumi Matsushige

Department of Electronic Science and Engineering, Kyoto University, Katsura, Nishikyo, Kyoto 615-8510, Japan

[1]Innovative Collaboration Center, Kyoto University, Katsura, Nishikyo, Kyoto 615-8520, Japan

[2]National Institute of Advanced Industrial Science and Technology, 1-1-1 Higashi, Tsukuba 305-8566, Japan

We demonstrated molecular resolution imaging of biological samples such as bacteriorhodopsin protein molecules in purple membrane and isolated chaperonin (GroEL) protein molecules, both adsorbed on mica using frequency modulation atomic force microscope (FM-AFM) in liquid. We also showed that the frequency noise of FM-AFM in liquid can be greatly reduced by the reduction of the noise-equivalent deflection of an optical beam deflection sensor.

----

* E-mail address: h-yamada@kuee.kyoto-u.ac.jp

†Present address: Frontier Science Organization, Kanazawa University, Kakuma, Kanazawa 920-1192, Japan

Atomic force microscopy (AFM) is a powerful imaging tool that can visualize biological systems in liquids. Among various imaging modes in AFM, contact-mode AFM has been mainly used for molecular resolution imaging of biological systems in liquids. A number of molecular resolution images of membrane proteins have been presented by contact-mode AFM[1]. However, the lateral motion of the tip in contact with the surface inevitably involves friction force. This makes it difficult to use contact-mode AFM for imaging isolated biomolecules weakly adsorbed on the substrate. This problem can be solved by the use of dynamic-mode AFM techniques. Amplitude-modulation AFM (AM-AFM) has been successfully applied for imaging biological samples[2]. On the other hand, a large number of true atomic and molecular resolution AFM images have been presented by the use of the frequency modulation (FM) method[3] in vacuum environments[4]. Since FM-AFM is also a dynamic-mode AFM technique, one can expect high-resolution imaging in liquid environments as well as that by AM-AFM[5-7]. However, liquid-environment FM-AFM is severely hindered by the extreme reduction of the cantilever Q-factor due to hydrodynamic interaction between the cantilever and the liquid. We recently developed an AFM apparatus with a low-noise optical beam deflection (OBD) sensor[8] and demonstrated true atomic resolution on muscovite mica by FM-AFM in pure water[9]. Non-destructive imaging of biological materials would require a much lower loading force than that for those samples. Therefore, showing the applicability of FM-AFM to soft biological systems is of great importance. Recently, one of the authors reported subnanometer-scale resolution FM-AFM imaging on isolated biological macromolecular assemblies on mica[10]. In this paper, we report our recent studies on noise analysis to show how does the reduction of the deflection sensor noise contribute to reduce on the frequency noise of the oscillator. Then we demonstrate molecular-resolution FM-AFM imaging of protein molecules such as bacteriorhodopsin (bR) in purple membrane and chaperonin (GroEL), which have been often studied by other operating modes, to show the advantages of the FM-AFM compared to those modes.

Figure 1 shows a schematic diagram of our FM-AFM setup. We used a modified commercial atomic force microscope (JEOL: JSPM-4200). Details of the modifications we have made were described elsewhere[8]. Thermal noise spectra of the cantilever were collected by a spectrum analyzer (Agilent Technologies: 4395A). Frequency noise spectra were measured by a fast Fourier transform analyzer

(Advantest: R9211B). In order to analyze an effect of the deflection sensor noise on the frequency noise, white noise signal from an arbitrary function generator (Tektronix: AFG3252) were added to the deflection signal. We used highly-doped n-type Si cantilevers (Nanosensors: NCH) whose k_z and f_0 were 40 N/m and 140 kHz in liquid, respectively. FM-AFM images were taken in the constant frequency shift mode where the tip-sample distance is controlled such that the frequency shift (Δf) of the cantilever resonance is kept constant. The cantilever was oscillated in the constant amplitude mode. The oscillation amplitude was about 1 nm peak-to-peak or less. The force sensitivity can be increased by the small-amplitude oscillation because of the increase in the effective duration of the proximity interactions.

Patches of purple membrane (PM) were collected from halophilic archaeon *Halobacterium salinarum*. In the purple membrane, bR protein molecules form a hexagonal lattice of trimers in a lipid bilayer matrix. PM patches were suspended in 100 mM KCl, 10 mM phosphate buffer solution (PBS) (pH 7.4). They were adsorbed onto a freshly-cleaved muscovite mica substrate by incubating solution on the mica for 20 min. Then the sample was gently rinsed with the buffer solution for removing non-adsorbed patches. FM-AFM imaging of PM was performed in the same buffer solution. Chaperonin 60, or GroEL protein molecules overexpressed in *Escherichia coli* was obtained as lyophilized powder from Sigma-Aldrich Corp. The powder was dissolved in buffer solution A (50mM HEPES-KOH, 100mM KCl, 5mM MgCl$_2$, 1mM dithiothreitol pH 7.5). A droplet of GroEL solution was applied onto a freshly cleaved muscovite mica. After incubation for 30 min, FM-AFM imaging was performed in buffer solution B (25 mM HEPES-KOH, 100mM KCl, 5mM MgCl$_2$, 10 mM DTT, pH 7.5).

GeomAFM Simulator software (Ver. 1.1) in SPM Sim Software suite[11] was used to simulate AFM images of GroEL protein molecules by calculating the tip trajectory when the outer surface of a conical tip touches and follows the outermost atoms of the protein molecules. We used a modeled tip with the half cone angle of 10 degree and the radius of the tip of 6 nm, and a protein model of GroEL from Protein Data Bank (PDB ID: 1GRL).

Figure 2(a) shows frequency spectra of the output signal from the OBD sensor measured when the NCH cantilever was immersed in water. The red curve shows that the noise-equivalent deflection for the cantilever was about 45 fm/$\sqrt{\text{Hz}}$, which was calculated by fitting to the thermal noise spectrum of the harmonic oscillator (black

curve). The Q-factor obtained as the best-fit parameter was about 9.5. Other colored curves such as blue, orange, purple, and green curves were measured with extra white noise added at the output of the OBD sensor. The noise-equivalent deflection density for those were measured as about 70, 100, 130, 220 fm/$\sqrt{\text{Hz}}$, respectively. We can see that it becomes very difficult to find the resonance frequency when the sensor noise becomes larger than 100 fm/$\sqrt{\text{Hz}}$. Figure 2(b) shows frequency spectra of the output of the frequency detector showing frequency noise density of the resonator when the cantilever was oscillated with an oscillation amplitude of 1 nm peak-to-peak. Each colored spectrum show the frequency noise density measured with the same condition as the spectrum with the same color in Fig. 2(a).

It has been known that the frequency noise density is proportional to the modulation frequency for high-Q cantilevers[12], however we found that it was independent of the modulation frequency and almost linearly increased with the magnitude of extra white noise. The frequency noise spectra were best fitted to the following equation,

$$\delta f = \sqrt{\frac{f_0 k_{\text{B}} T}{2\pi k_z Q A_{\text{rms}}^2} + \left(\frac{f_0}{2Q}\frac{n_{\text{ds}}}{A_{\text{rms}}}\right)^2},$$

where A_{rms} and n_{ds} are the root-mean-squared amplitude of the cantilever and the noise-equivalent deflection density, respectively. k_{B} and T are the Boltzmann constant and the temperature. The frequency noise densities calculated by the above equation were indicated as dotted lines. The first term is the intrinsic frequency noise of the oscillator when the deflection sensor noise is negligibly small[3]. The second term is understood as follows. In the self-oscillation loop, the phase noise of the oscillator $\delta\phi = n_{\text{ds}}/A_{\text{rms}}$, is converted to the frequency noise by the factor of $f_0/2Q$, which is a slope of the slope of the frequency resonance of the phase of the cantilever $|df/d\phi|$ at the resonance frequency. The frequency noise spectra in Fig. 2(b) show that the signal-to-noise ratio in the frequency signal was greatly affected by the deflection sensor noise. The second term becomes dominant when the noise-equivalent deflection density exceeds $\sqrt{2k_{\text{B}}TQ/\pi k_z f_0}$, which was about 70 fm/$\sqrt{\text{Hz}}$, in this case. The measurement presented here shows that the contribution of the OBD sensor noise to the frequency noise is larger than that expected from the noise analysis for high-Q cantilevers, therefore the reduction of the noise-equivalent deflection in the deflection

sensor is essentially important especially in the low-Q environments.

Figure 3 shows FM-AFM images of a PM on mica in the PBS. Figure 3(a) shows a large-scale structure of the PM. The hexagonal arrangement of bR trimers is visible all over the membrane including at its fringe. Figure 3(b) shows a more magnified image where individual bR molecules are resolved. Considering the symmetry of the bright spots, the membrane is a cytoplasmic side while the extracellular side attached to the mica. The areas marked with white squares are enlarged in Figs. 3(c) and 3(d). While Fig. 3(c) shows a complete bR trimer, Fig. 3(d) presents the one with a single molecular defect. The images obtained here are still not as fine as those obtained by the contact-mode AFM[2], however, it is comparable to those obtained by the AM-AFM[8,9] and we believe that the resolution of the images can be improved by the further optimization of the imaging parameters. We also measured the frequency shift versus tip-sample distance curves as shown in Fig. 3(d). Figure 3(e) is the force versus distance curves by the method proposed by Sader and Jarvis[13], showing that the typical force exerted by the tip during imaging with typical imaging conditions was below than 100 pN. One of the advantages of the FM-AFM is that it is possible to quantitatively measure and control the applied loading force as demonstrated here.

Figure 4(a) shows FM-AFM images of GroEL protein molecules adsorbed on mica in the buffer solution B. A GroEL is a tetradecamer molecule, where 7 identical subunits forms a donut-like heptamer and the two heptamer are facing each other. The apparent size of the individual GroEL molecules observed in the lower part in Fig. 4(a) was about 14 nm in diameter and 14 nm in height. On the other hand, the height of some molecules in the upper part was about 7 nm. These molecules are bottom heptamer molecules exposing equatorial domains, whose top heptamers were probably scraped off by a relatively high loading force or frictional force. Figure 4(b) and 4(c) shows FM-AFM images showing fine structures of the GroEL molecules exposing the outer surface (apical domain) of the tetradodecamer unit and equatorial domains of the bottom heptamer, respectively. We show simulated AFM images in the lower right of the two images. As expected in the AFM image, the apical domain of the molecule appears like a flower with seven petals. Note that the individual subunits are nearly resolved in the AFM image. On the other hand, the AFM image of the equatorial domain in Fig. 4(c) appears like a circle with a hole with a shape of a circle or a star.

This contrast is also well corresponded to the simulated AFM image.

Since the GroEL molecules were weakly attached onto the mica substrate, it has been very difficult to obtain high-resolution images of apical domain of the GroEL molecules by the contact-mode AFM and the AM-AFM. Only a few research groups have successfully obtained high-resolution images of the apical domain of the GroEL by fixing the molecules tightly to the substrate by glutaraldehyde[14] or the apical domain of the heptamer mutant GroEL-SR1 on graphite[15]. The apparent depth of the center hole in one of the previous studies was about 0.5 nm[15], whereas it was typically more than 1 nm in this study, as shown in a cross-sectional line profile measured across the center of the specific GroEL molecule indicated by the arrow in Fig. 4(b). The line profile taken from the simulated image in the inset of Fig. 4(b) is also shown as a grey thick curve in Fig. 4(d). The depth of the center hole in the simulated image was also about 1 nm. Therefore we believe that the FM-AFM images obtained here were taken at a lower loading force than that in the previous studies and the resolution was better than those.

In summary, we measured the relationship between the deflection sensor noise and the frequency noise of the self-oscillated cantilever and showed the importance of the reduction of the deflection sensor noise in the FM-AFM operated in liquid. We also showed molecular-resolution images of membrane proteins (bacteriorhodopsion) and isolated proteins (GroEL) adsorbed on mica. This demonstrates the applicability of FM-AFM to biological systems.

References

1) D. J. Müller, G. Büldt, and A. Engel: J. Mol. Biol. **249** (1995) 239.

2) C. A. J. Putman, K. O. van der Werf, B. G. de Grooth, N. F. van Hulst, J. Greve, Biophys. J. **67** (1994) 1749.

3) T. R. Albrecht, P. Grütter, D. Horne, and D. Rugar: J. Appl. Phys. **69** (1991) 668.

4) *Noncontact Atomic Force Microscopy* (Springer, Berlin, 1997), eds. S. Morita, R. Wisendanger, and E. Meyer.

5) C. Möller, M. Allen, V. Elings, A. Engel, and D. J. Müller, Biophys. J. **77** (1999) 1150.

6) H. Yamashita, K. Voïtchovsky, T. Uchihashi, S. A. Contera, J. F. Ryan, and T. Ando, J. Struct. Biol. **167** (2009) 153.

7) J. Preiner, J. Tang, V. Pastushenko, and P. Hinterdorfer, Phys. Rev. Lett. **99** (2007) 046102.

8) T. Fukuma, M. Kimura, K. Kobayashi, K. Matsushige, and H. Yamada: Rev. Sci. Instrum. **76** (2005) 053704.

9) T. Fukuma, K. Kobayashi, K. Matsushige, and H. Yamada: Appl. Phys. Lett. **86** (2005) 193108.

10) T. Fukuma, A. S. Mostaert, L. C. Serpell, and S. P. Jarvis, Nanotechnology **19** (2008) 384010.

11) SPM Sim Software suite was developed by Prof. M. Tsukada and coworkers, under SENTAN Program of the Japan Science and Technology Agency.

12) U. Dürig, H. R. Steinauer, and N. Blanc, J. Appl. Phys. **82** (1997) 3641.

13) J. E. Sader and S. P. Jarvis, Appl. Phys. Lett. **84** (2004) 1801.

14) J. Mou, S. Sheng, R. Ho, and Z. Shao, Biophys. J. **71** (1996) 2213.

15) J. Schiener, S. Witt, M. Hayer-Hartl, R. Guckenberger, Biochem. Biophys. Res. Commun. **328** (2005) 477.
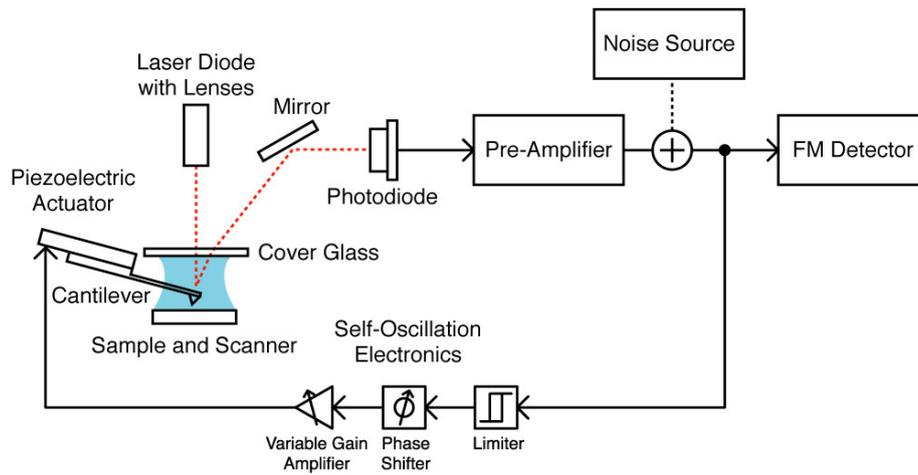
Figure 1: Schematic of frequency-modulation AFM in liquid.

(a)	(b)
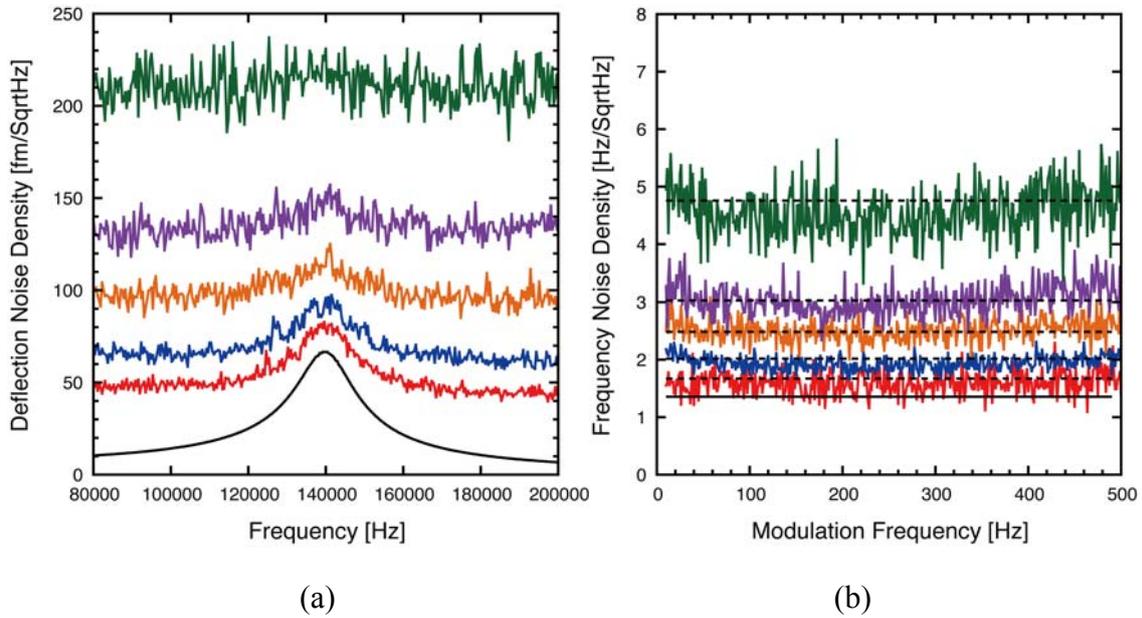
Figure 2: (a) Deflection noise density spectra of a cantilever (NCH) in liquid. Red curve is a spectrum without extra white noise (45 fm/$\sqrt{\text{Hz}}$). Other colored curves were measured with extra white noise. (b) Frequency noise density spectra measured when the cantilever was oscillated with an oscillation amplitude of 1 nm peak-to-peak.

9
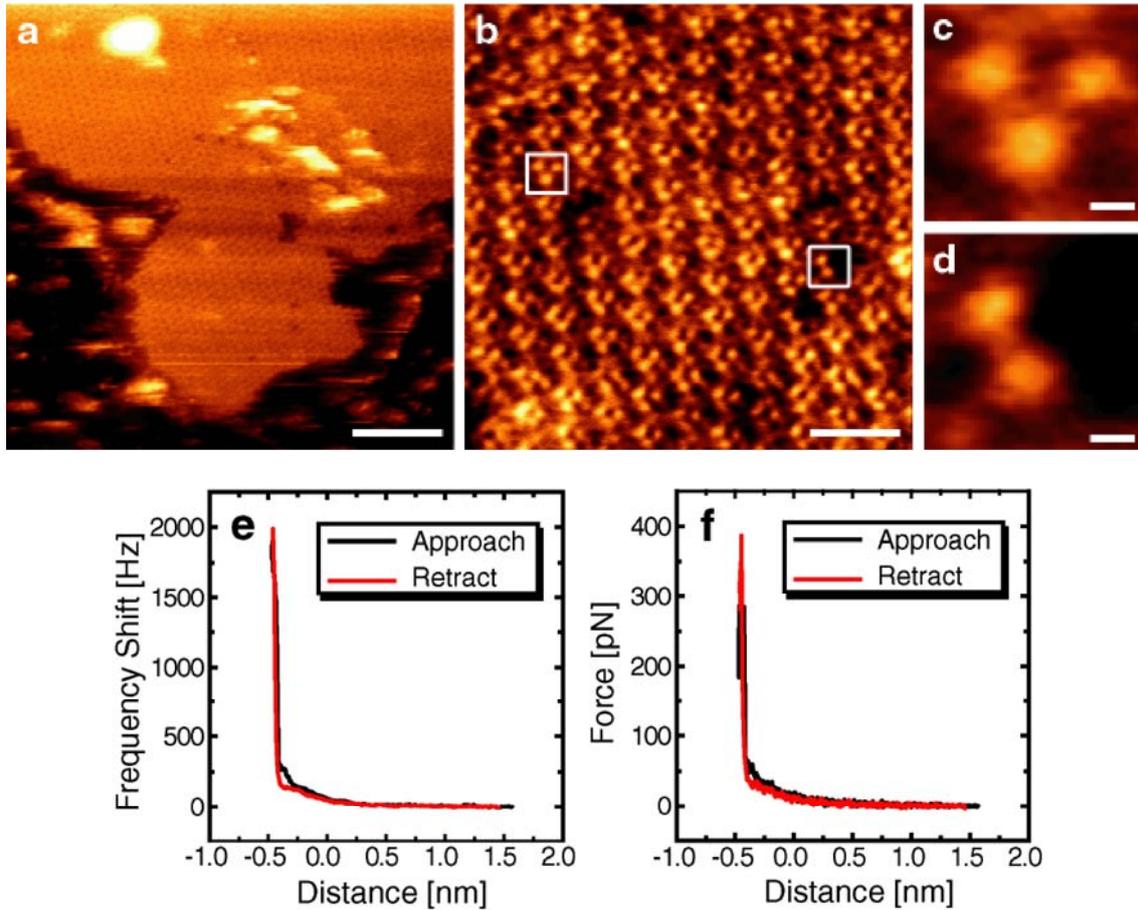
Figure 3: FM-AFM images of a purple membrane including bacteriorhodopsin protein molecules adsorbed on muscovite mica in phosphate buffer solution. (a) Scale bar: 60 nm, $A = 0.12$ nm, $\Delta f = 160$ Hz. (b) Scale bar: 16 nm, $A = 0.55$ nm, $\Delta f = 283$ Hz. (c), (d) Scale bars: 1.4 nm. Figs. 3(c) and 3(d) are the magnified images of the areas indicated by the white squares in Fig. 3(b). (e) Frequency shift versus tip-sample distance curve measured on purple membrane. (f) Force versus tip-sample distance curve derived from (e).
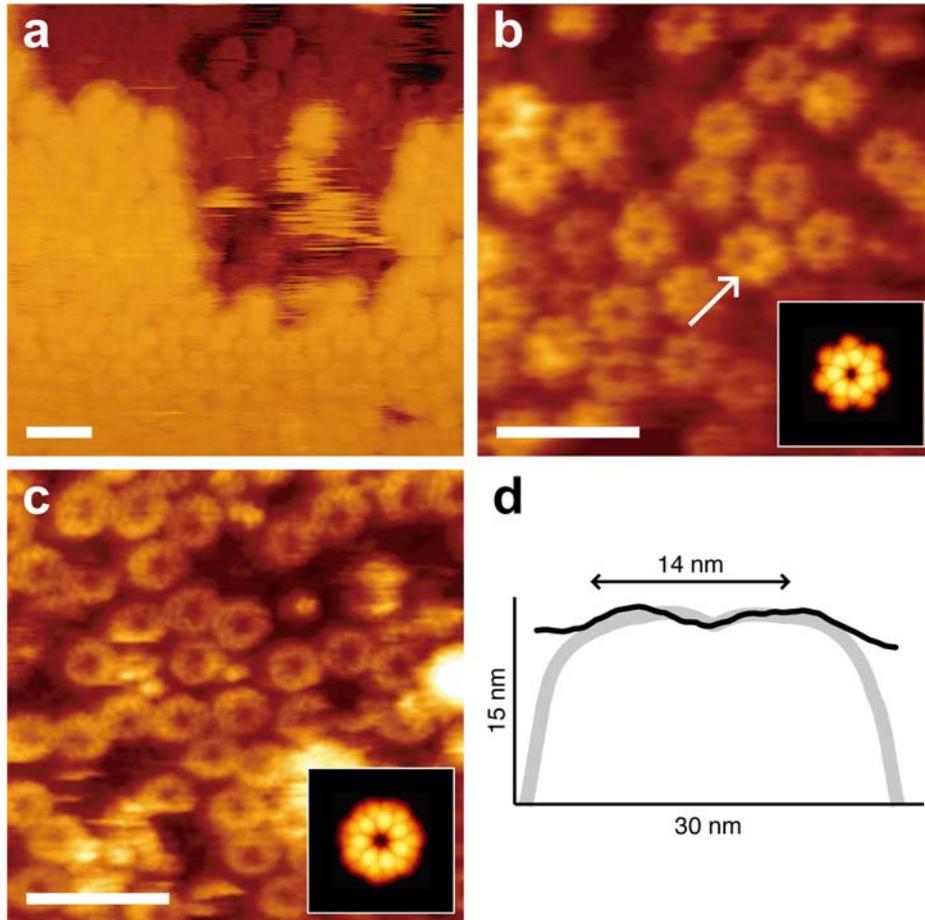
Figure 4: (a) FM-AFM images of chaperonin protein molecules attached on muscovite mica in HEPES buffer solution. Scale bar: 50 nm, $A = 0.8$ nm, $\Delta f = 110$ Hz. (b) and (c) are FM-AFM images apical domain and equatorial domain, respectively. Scale bars: 50 nm, $A = 0.5$ nm, $\Delta f = 50$ Hz. Simulated AFM images were shown in the insets (Simulated scan area: 30 nm). (d) Cross-sectional line profile measured across the center of the GroEL molecule indicated by the arrow in (b) and that taken from the simulated image in the inset of (b).